Power and Bandwidth Allocation based on Age of Information metrics in Satellite Uplink Channels

Jorge Torres Gómez*, Maximo Morales-Céspedes†, Musbah Shaat‡, Ana I. Pérez Neira§, Ana García Armada¶

*School of Electrical Engineering and Computer Science, TU Berlin, Germany,
†¶Department of Signal Theory, University Carlos III of Madrid, Leganés, Madrid, Spain,
‡§Dept. Signal Theory and Communications - Universitat Politecnica de Catalunya (UPC), Barcelona, Spain,
§Centre Tecnologic de Telecomunicacions de Catalunya (CTTC/CERCA), Castelldefels, Barcelona, Spain
*torres-gomez@ccs-labs.org, †mmcesped@ing.uc3m.es, ‡musbah.shaat@cttc.es, §ana.perez@cttc.es, ¶agarcia@tsc.uc3m.es

Abstract—Communication links over satellites allow interconnecting very distant regions to provide service where the terrestrial networks are limited. In this scenario, it is of major importance to devise mechanisms accounting for the improved freshness of packets given the impact of large distances. Their analysis is particularly important when considering the deployment of sensors in remote areas, where satellite links may introduce a high delay in the communication system. In this respect, we report the use of age of information (AoI) metrics to evaluate users' allocation mechanisms. We use power-domain non-orthogonal multiple access (NOMA) as an alternative to orthogonal multiple access (OMA) to optimally reduce the age of received packets. We derive the proper formulation to account for a fairness condition when pairing users accounting for both; the user's needs to transmit information and the allowable link rate. Comparative results are provided by numerically evaluating the solution for NOMA and OMA. We show that the standard user allocation in NOMA, that is, users of very distinct channel gain are paired, does not result in less age of information when users are paired according to a similar channel condition or when guaranteeing a minimum sum-rate per users' pairs. We remark this result through extensive numerical simulations based on actual uplink satellite communication links accounting for 500 users.

I. Introduction

Satellite communication links provide the means for the coverage of terminals over wide areas at very distant regions, where the deployment of terrestrial networks is typically limited. Nowadays, terrestrial networks do not support services over the 80 % of the world's lands and 90 % of the world's ocean, where the satellite system can naturally provide services [1]. The broad coverage provided by satellites also accounts for the implementation of ubiquitous communication networks, achieving data rates around 100 Gbit/s per second [2], since the connection of users in those remote areas is provided.

Through satellite communication systems, the use of power-domain non-orthogonal multiple access (NOMA) is particularly suited [3] provided its fulfillment of heterogeneous requirements such as throughput, low latency, and high-reliability [4], [5]. Besides, NOMA provides enhanced spectrum efficiency when compared to the usual implemented orthogonal multiple access (OMA), which becomes particularly important with large number of connections in satellite systems [6].
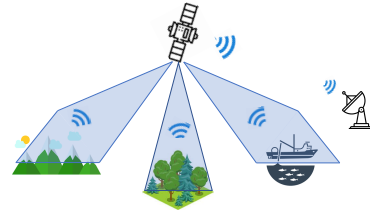

Figure 1: Illustration of the satellite system to support IoT applications

A variety of solutions are reported to implement resource allocation mechanisms in satellite links through NOMA. Power control mechanisms can be implemented to provide quality of service (QoS) in terms of the node rate [7], and also considering restrictions such as the satellite's power [8], the power per transmitted antenna in the user side [9], and imperfect channel state information (CSI) [10]. Solutions are also reported to fairly allocate users per satellite beam to maximize their achievable sum-rate [11], and with improved performance in comparison to OMA when maximizing throughput [12]. Additionally, energy-efficient solutions can be devised by implementing a resource allocation mechanism to maximize the ratio of achievable capacity to energy consumption [13].

In a different approach, here we apply the age of information (AoI) concept in satellite uplink channels to implement resource allocation mechanisms. The AoI accounts for the freshness of the collected information at a given destination node regarding remote sensors' sources [14]. In this respect, this concept will play a major role to devise solutions in satellite networks that support the next industrial internet of things (IIoT), for instance [15]. Their applicability directly concerns forest harvesting, marine development, video surveillance, and geological explorations [1], as illustrated in Fig. 1.

Considering a remote fusion center to collect the status updates of terrestrial terminals (as described in Section II), our goal is to reduce the perceived average peak age of information (PAoI) ta the destination node (cf. Section III). To that end, we provide insights to compute optimal power and bandwidth allocation for groups of two users. We comparatively analyze the

impact of NOMA and OMA and the corresponding resource allocation mechanisms, i.e. bandwidth and power levels for users paired according to OMA and NOMA, respectively. We illustrate results and discuss three different users' pairing rules for the NOMA scheme (cf. Section IV).

II. SYSTEM MODEL

We consider a high throughput satellite (HTS) in geostationary orbit providing multiple beams in the downlink. For each beam, we focus on uplink transmission in which N terrestrial terminals (so-called users) send information a destination node D, as shown in Fig. 2. Moreover, the considered users are located within the same beam of the HTS so that the interference with other users in distinct beams can be considered negligible. Specifically, the communication system comprises the following elements:

- **Source node:** Denoted by s_i with packet generation-rate λ_i and information entropy H_i.
- **Transmitter:** Each transmitter comprises a queue where the packets from the source node are queued according to a first-come-first-served (FCFS) discipline. The M/M/1 queuing system is assumed to model the packet arrivals according to a Poisson process and exponential service time to deliver the packets from the queue. The performance of each transmitter k is determined by its transmission power and packet rate denoted by P_k and μ_k, respectively. Notice that the rate μ_k also denotes the service rate of the queue.
- **Channel:** The downlink path is assumed ideal and only the propagation delay is considered, which corresponds to $T_d = 125$ ms approximately. The uplink channel is located in Ka band and the propagation loss for user k is modeled as [16]

$$h_k = \frac{AG_T g_k}{4\pi \frac{d_k}{\lambda_c}\sigma} \quad k = 1,\ldots,N, \tag{1}$$

where A corresponds to the loss due to atmospheric fading, G_T is antenna gain of the user terminals, g_k refers to the gain from the receiving beam pattern at the satellite, which depends on the location of the user terminal, d_k is the distance between the k-th user and the satellite, λ_c is the carrier wavelength.
Furthermore, the channel gain h_k is normalized to the square root of the noise power denoted by σ. Given h_k, the input-output relation for a particular time instant can be written as

$$y_k = h_k s_k + n_k, \tag{2}$$

where s_k is the transmitted sample for user k, and n_k is the additive white gaussian noise (AWGN) with spectral density N_0.
- **Multiple Access:** Collisions in the uplink are avoided through resource allocation mechanisms. Besides, switching between NOMA and OMA transmissions is considered. As it is shown in Fig. 2, several users are served
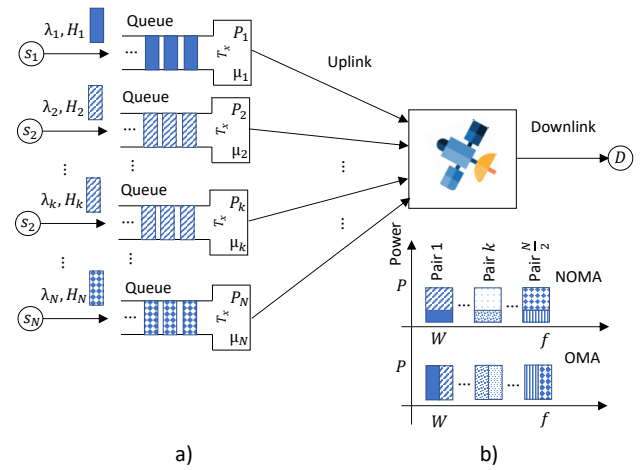

Figure 2: Illustration of the uplink satellite communication system.

in the same bandwidth W if power-domain NOMA is selected, while the users are served in orthogonal frequency slots along the bandwidth W for OMA transmission.
- **Destination Node:** Denoted by D, this node collects the packets transmitted by the source nodes.

III. RESOURCE ALLOCATION UNDER AoI CONSTRAINTS FOR SATELLITE COMMUNICATIONS

The AoI corresponds to the status update at the destination concerning each packet transmitted from the source. Once the packet arrives, the AoI function measures the elapsed time since it was generated [14]. Therefore, its corresponding metrics, like average AoI and the PAoI, can be interpreted as the freshness of information. Specifically, here we address resource allocation mechanisms to minimize the average PAoI metric. This metric results in better mathematical tractability than the average AoI, since it avoids the cumbersome computation of cross-terms statistics. Similar to the average AoI metric, the average PAoI captures the trade-off between system load and rate of emissions.

Having into account the impact of delivery errors, produced by the channel noise, we assume the formulation provided in [17] for the average PAoI as

$$\Delta_k^{(p)} = \frac{1}{(1-\text{SER})\lambda_k} + \frac{1}{\mu_k - \lambda_k} + T_d, \tag{3}$$

where we include the term T_d for the propagation delay, SER is the symbol error rate, k denotes the user, and $\mu_k > \lambda_k$ in order to guarantee the stability of the system. Notice that the average PAoI can be decomposed into the expected inter-arrival time between two packets received successfully, which is given by $\frac{1}{(1-\text{SER})\lambda_k}$, plus the time a packet spends on the system due to the delay introduced by the queues and the propagation, given by $\frac{1}{\mu_k - \lambda_k} + T_d$.

However, the PAoI, as formulated in (3), does not consider a resource allocation mechanism for unequal channel conditions and source entropies among users [18]. To do so, we include

the ratio of the source entropy, denoted as H_k, to the allowable total bits per channel use, denoted as R_k, yielding

$$\Delta_{k_{H,R}}^{(p)} = \frac{H_k}{R_k}\left(\frac{1}{(1-\text{SER})\lambda_k} + \frac{1}{\mu_k - \lambda_k} + T_d\right), \quad (4)$$

where $R_k = \log_2(1+\text{SNR}_{k,\Gamma})$, $\text{SNR}_{k,\Gamma} = \frac{h_k P_k}{\Gamma N_0 W_k + P_j}$ is the signal-to-noise ratio when the user k is the ones with the higher power level for NOMA users, otherwise $\text{SNR}_{k,\Gamma} = \frac{h_k P_k}{\Gamma N_0 W_k}$ (including OMA users), and Γ is the SNR-gap factor to account for reliable links [19]. Implicitly, it is assumed on this formulation the use of successsive-interference-cancellation (SIC) receivers to decode NOMA users [20].

The term $\frac{H_k}{R_k}$ in (4) allows us to determine the average number of channel accesses required per emitted bit of information. Users with poor channel conditions (low R_k) or a high demand to transmit information (high H_k) lead to a high $\frac{H_k}{R_k}$ ratio, which in turn will request for more channel accesses than those users with a low $\frac{H_k}{R_k}$ ratio. Consequently, optimizing (4) takes into consideration user fairness when implementing resource allocation mechanisms. From now on, by using (4) we evaluate the impact of resource allocation for NOMA and OMA concerning the average PAoI.

A. The impact of NOMA and OMA in the average PAoI metric

Considering the system model depicted in Fig. 2, NOMA transmission assumes that up to N users can be paired in the same frequency band W over the power domain. For OMA transmissions, an orthogonal frequency slot comprising a bandwidth equal to W is allocated to each user for a transmission power equal to P. Under these assumptions, we focus on determining the performance of NOMA and OMA to minimize the average PAoI for the worst-case user as

$$\min_{\lambda_k, P_k, \mu_k}\max\left[\frac{H_k}{R_k}\left(\frac{1}{(1-\text{SER})\lambda_k} + \frac{1}{\mu_k - \lambda_k} + T_d\right)\right], \quad (5)$$
$$\text{s.t.:} \quad P_k \leq P, \lambda_k \leq \mu_k, \mu_k \leq \frac{W}{2},$$

where W is the channel bandwidth that limits the packet rate μ_k.

In the case of NOMA, the proposed min-max formulation minimizes the worst-case user by properly controlling the user rate λ_k and transmission power P_k parameters, where it is assumed the largest bandwidth per user i as $\mu_k = \frac{W}{2}$. In the case of OMA, the user and service rate parameters, λ_k and μ_k respectively, are optimized by assuming the largest transmission power $P_k = P$ per user.

For NOMA transmissions, considering that $\mu = \mu_k = \frac{W}{2}$ is constant, after factoring out μ_k from the second term in (5) yields

$$\min_{\lambda_k, P_k}\max \Delta_{k_{H,R}}^{(p)} = M_k \cdot (A_k + C) \quad (6)$$

where

$$M_k = \frac{H_k}{\mu R_k} = 2\frac{H_k}{W R_k}, \quad (7)$$

$$A_k = \frac{1}{(1-\text{SER})\rho_k} + \frac{1}{1-\rho_k}, \quad (8)$$

$$C = \mu T_d = \frac{1}{2}W T_d, \quad (9)$$

and $\rho_k = \frac{\lambda_k}{\mu}$ is the system utilization.

By this arrangement of terms, a solution can be formulated when solving for the two factors, separately. The factor M_k will be only dependent on the transmission power P_k, while the factor $(A_k + C)$ will be only dependent on the transmission rate λ_k, since the term C remains constant independently of the user parameters λ_k and P_k. Besides, the optimal value of A_k in (8) can be determined following [17] in terms of ρ^* for a given SER, which in turn provides the optimal solution for a user rate given by $\lambda_k^* = \mu \rho^* = \frac{W}{2}\rho^*$. At this point, it is worth noticing that the problem formulation for NOMA is reduced to analyze the factor M_k in (7) only.

If OMA transmissions are considered, the impact of μ_k cannot be isolated from the objective function in (5). This issue can be easily checked since μ_k cannot be managed independently from λ_k. Thus, the optimization problem must jointly determine both values μ_k and λ_k.

In the following, we focus on analyzing the solution to (5) to devise an optimal resource allocation mechanism. Specifically, we consider two steps that determine the performance of both OMA and NOMA transmissions. First, we address a solution to (5) per frequency band, i.e. given a pair of users, we conceive a method to derive the frequency band and the power level per user (cf. Fig. 2 b)). Then, the user pairing rules are analyzed so that we can determine the users allocated to each frequency slot, which comprises a bandwidth W.

B. Resource allocation per frequency band

The resource allocation problem per frequency band is referred to the power level assigned to each user pair (in case of NOMA), or the bandwidth (in case of OMA) to minimize the average PAoI metric. As depicted in Fig. 3, two users allocated on a given frequency band (W), will exhibit different average PAoI metrics according to their assigned resources. The user with the most resources (bandwidth or power) will present the lowest metric. Following this picture, the optimal solution to the min-max formulation will be attained in the interception of the two curves by solving the condition $\Delta_{i_{H,R}}^{(p)} = \Delta_{j_{H,R}}^{(p)}$.

For NOMA transmissions, managing the power allocated to each user is equivalent to handling the parameter M_k in (7). Following this approach, the optimal solution corresponds to evaluating the condition $M_i = M_j$ yielding

$$\frac{H_i}{R_i} = \frac{H_j}{R_j}, \quad (10)$$

The equation in (10) can be also represented in the capacity region of both users. As it is shown in Fig. 4, providing the same rate for both users corresponds to a line with slope equal to H_i/H_j. Thus, the proposed problem is reduced to determine
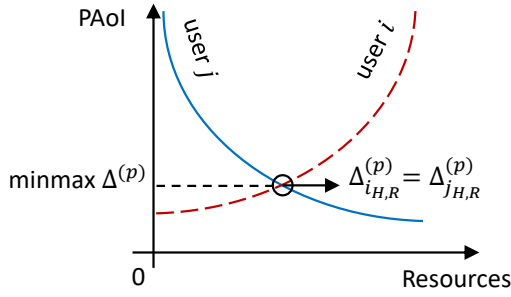
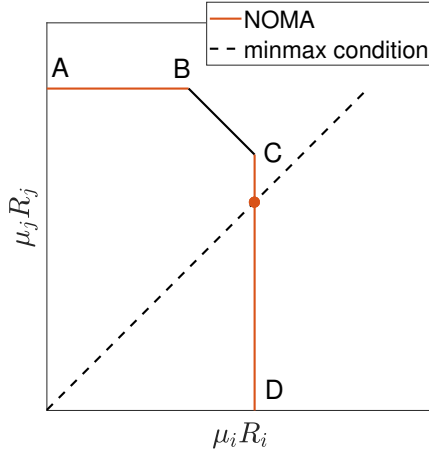Figure 3: Trade-off illustration of the two-user resource allocation case

Figure 4: Capacity region of NOMA for the two users case.

the intersection of this line with the capacity region subject to (10).

We should consider that the interception point can be located in three distinct segments of the capacity region (see Fig. 4). If the interception occurs in the segment CD, user j must be decoded first treating the signal of user i as interference. After that, SIC is carried out so that the decoded symbol from user j is used to cancel the interference due to its transmission when decoding the symbol intended to user i. On the other hand, if the interception is located within the segment AB, the opposite case must be implemented, i.e., user i is decoded treating user j as interference. Finally, if the intersection is located in the segment BC, time-sharing or rate-splitting resource allocation can be applied. In particular, we implement a time-sharing solution to address such cases.

In the case of OMA, we solve for each user pair the optimal $\frac{W_i}{W_j}$ ratio value through (4) as $\Delta_{i_{H,R}}^{(p)} = \Delta_{j_{H,R}}^{(p)}$ for W_i, W_j, λ_i, and λ_j, and considering $P_k = P$. This must be solved numerically to assign the optimal bandwidth for each user on each corresponding pair.

C. User pairing

A variety of user pairing mechanisms have been developed for NOMA transmissions [21]. Most common solutions are the next-largest-difference-based user pairing algorithm (NLUPA) to maximize the sum-rate, the cognitive radio (CR)-inspired to

guarantee the QoS of the weak user, and the divide and -next-largest-difference-based user pairing algorithm (D-NLUPA) to guarantee a minimum sum-rate gain for each users' pairs (cluster fairness). In this work we adopt these three different user pairing methods to evaluate the resulting average PAoI metric.

In the case of NLUPA, basically, each user is paired with the user that corresponds to the largest channel difference. Assuming that users are sorted so that $|h^{(1)}| < |h^{(2)}| < \cdots < |h^{(N)}|$, the following user pairing criterion is applied

$$\text{Rule 1: } \left(|h^{(1)}|, |h^{(N)}|\right), \left(|h^{(2)}|, |h^{(N-1)}|\right), \quad (11)$$
$$\cdots, \left(|h^{(\frac{N}{2})}|, |h^{(\frac{N}{2}+1)}|\right),$$

where we recall that $h^{(k)}$ is given by (1).

However, considering the solution for the min-max problem depicted in Fig. 3, the users with poor channel conditions are penalized by users with a better gain. As a consequence, pairing the users with similar channel conditions results suitable in order to minimize the average PAoI. Under this reasoning, users are paired according to the following criterion

$$\text{Rule 2: } \left(|h^{(1)}|, |h^{(2)}|\right), \left(|h^{(3)}|, |h^{(4)}|\right), \quad (12)$$
$$\cdots, \left(|h^{(N-1)}|, |h^{(N)}|\right),$$

by pairing users with similar channel condition (CR-inspired).

Finally, Rule 3 follows the D-NLUPA mechanism [21], where users are divided into four sets after sorting according to the channel gain. Then, pairs of sets are merged in such a way that a minimum channel gain difference is guaranteed. In our case, the first set is merged with the third, and the second one with the last one, similar to the diagram in Fig. 2 [21]. Following this ordering, the standard NLUPA mechanism is applied.

IV. NUMERICAL RESULTS

A satellite uplink comprising 500 users is considered for providing simulation results. It is assumed that all the users generate the same information entropy, i.e., $H_i = H_j \,\forall_{(i,j)}$, the available bandwidth is 20 MHz, the maximum power per user terminal is 2 Watts and the required SER without channel coding is equal to 10^{-5}.

Fig. 5 depicts the resulting user pairing rules NOMA according to Rule 1 in (11), Rule 2 in (12), and Rule 3 are considered. It can be seen that Rule 1 is subject to a varying performance because of the great disparity between users, i.e., users with high channel gain are paired to users with low gain. Indeed, this variation becomes smaller for larger users' pairs. The Rule 2 provides a decreasing monotonic curve with the pairing index as users with high channel gain are located in the first user pairing indexes. In the case of Rule 3, it can be observed that a minimum channel difference is guaranteed between users. i.e. users 249 and 250 have not equal channel gain as the case of rules 1 and 2.

To illustrate the resource allocation of OMA and NOMA access schemes, we derive the proper bandwidth per user
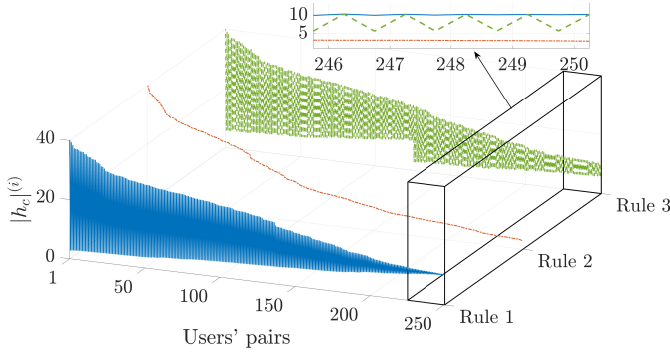
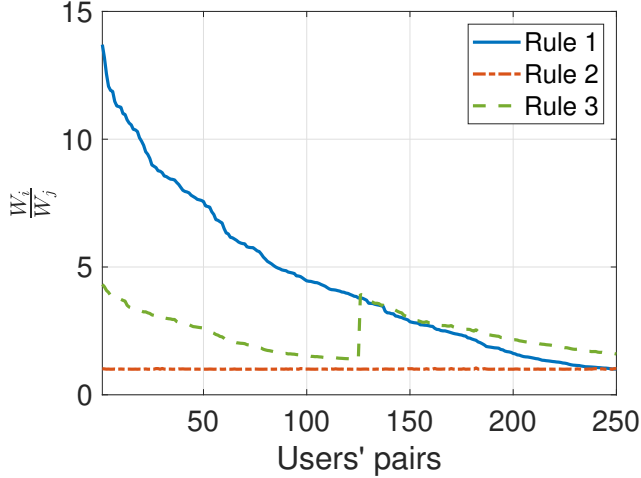Figure 5: User pairing rules according to their channel gains.

Figure 6: Resulting resource allocation in OMA regarding the two rules to pair users.
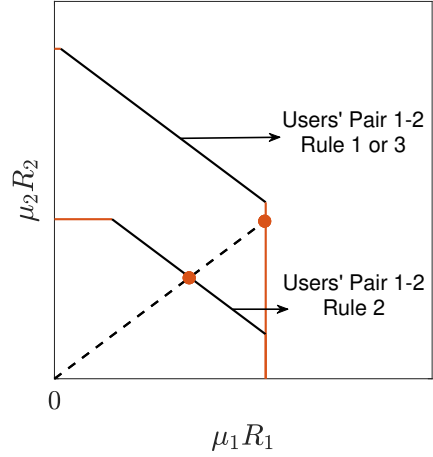

Figure 7: Interception point for the NOMA users's pairs through the Rules 1 and 2.
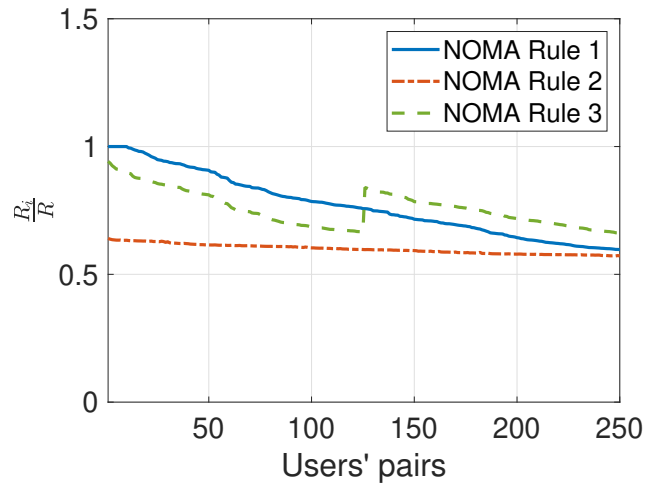
Figure 8: Resulting resource allocation in NOMA regarding the two rules to pair users.

and the order to implement the SIC receiver, respectively as described in Section III. As depicted in Fig. 6 for OMA transmissions, the Rule 1 favors those users with the worst channel condition. Besides, this bandwidth distribution tends to be symmetrically distributed as both users' channel-gains get close to each other. In the case of Rule 2, the bandwidth distribution is almost equally shared for all the users' pairs. This is in correspondence with the similar user channel gain that each pair of users has. In the case of Rule 3, the bandwidth assignment presents an abrupt change following the non-symmetrical ordering of users, and the resulting bandwidth allocation is also in favor of users with the worst channel condition.

In the case of NOMA, we evaluate the optimal user ordering when implementing the SIC receiver. To illustrate this, Fig. 7 depicts the interception points for the three rules. Regarding the pair (1-2) in the Rule 1 or 3, where the channel condition is distinct, the solution is derived in favor of the user 1 (worst channel condition). The ordering for the SIC receiver will be to decode user 2 first and then user 1. Regarding the user's pairs for the Rule 2, where the channel condition is approximately equal, the interception point is located in the time-sharing region. In this case, the user ordering to implement SIC must be proportionally interchanged.

The impact of the user pairing in the proposed schemes is determined by the interception point in which R_i equals R_j as shown in Fig. 4. The percentage of time the user i will be decoded in the second stage can be directly computed as a ratio of the achievable rate R_i to their maximum rate $R = \log_2(1 + \frac{h_{c,i}P}{\Gamma N_0 W})$. This resulting ratio is depicted in Fig. 8 for the two rules. For the three rules, the user with the worst channel condition is favored on each pair. More than fifty percent of the time it will be decoded in the second stage avoiding the interference produced by the corresponding paired user.

To compare the resulting average PAoI for both access schemes, Fig. 9 illustrates the outcomes for the three rules. The resulting pairing rules achieve a PAoI between 0.032 s and 0.073 s, which accounts for the minimimum average PAoI per users' pairs. That is, events happening at the source will be perceived at the destination side with a maximum age around this value. On each rule, NOMA exhibits improved performance regarding the average PAoI reduction in comparison to OMA. However, in the case of Rule 2, NOMA and OMA
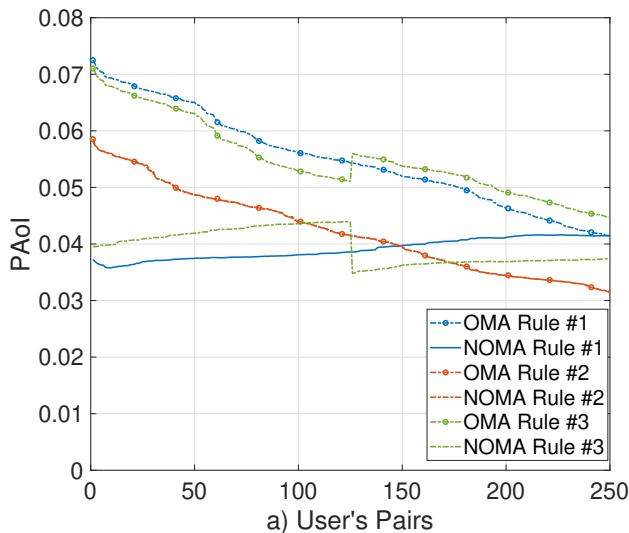
Figure 9: Resulting average PAoI for NOMA and OMA access schemes. a) Rule 1. b) Rule 2.

exhibit nearly equal performance provided that both users have nearly equal channel gains.

Furthermore, considering similar results, the Rule 2 provides a metric to compare the best performance of OMA vs NOMA. By comparing the three rules in Fig. 9, neither method will exhibit such a distinct performance regarding a reduced average PAoI. More generally, a users' pairing rule that best captures the benefits of these rules is still to be derived considering an arbitrary channel gain distribution.

V. Conclusion

This work provided results regarding the average PAoI as a metric to implement user allocation mechanisms in uplink satellites. The applied PAoI metric allowed to optimize for the freshness of information, which accounts for applications where remote sensors are deployed. Considering the user's links in the uplink satellite, the status update about remote sensors will be around the 0.05 s. Besides, regarding the pairing rules, results inferred that there is an optimal user pairing mechanism that best captures the results of both. Further research will be conducted to analyze the optimal users' pairing rule. Future work will be also conducted to analyze resource allocation algorithms with imperfect CSI and heterogeneous terminals.

References

[1] X. Liu, X. B. Zhai, W. Lu, and C. Wu, "QoS-Guarantee Resource Allocation for Multibeam Satellite Industrial Internet of Things With NOMA," *IEEE Transactions on Industrial Informatics*, vol. 17, no. 3, pp. 2052–2061, Mar. 2021.

[2] A. I. Perez-Neira, M. A. Vazquez, M. R. B. Shankar, S. Maleki, and S. Chatzinotas, "Signal Processing for High-Throughput Satellites: Challenges in New Interference-Limited Scenarios," *IEEE Signal Processing Magazine*, vol. 36, no. 4, pp. 112–131, Jul. 2019.

[3] X. Zhu, C. Jiang, L. Kuang, N. Ge, and J. Lu, "Non-Orthogonal Multiple Access Based Integrated Terrestrial-Satellite Networks," *IEEE Journal on Selected Areas in Communications*, vol. 35, no. 10, pp. 2253–2267, Oct. 2017.

[4] W. Shin, M. Vaezi, B. Lee, D. J. Love, J. Lee, and H. V. Poor, "Non-Orthogonal Multiple Access in Multi-Cell Networks: Theory, Performance, and Practical Challenges," *IEEE Communications Magazine*, vol. 55, no. 10, pp. 176–183, Oct. 2017.

[5] A. I. Perez-Neira, M. Caus, and M. A. Vazquez, "Non-orthogonal transmission techniques for multibeam satellite systems," *IEEE Communications Magazine*, vol. 57, no. 12, pp. 58–63, 2019.

[6] X. Yan, K. An, T. Liang, G. Zheng, Z. Ding, S. Chatzinotas, and Y. Liu, "The Application of Power-Domain Non-Orthogonal Multiple Access in Satellite Communication Networks," *IEEE Access*, vol. 7, pp. 63 531–63 539, 2019.

[7] H. Liu, T. A. Tsiftsis, K. J. Kim, K. S. Kwak, and H. V. Poor, "Rate Splitting for Uplink NOMA With Enhanced Fairness and Outage Performance," *IEEE Transactions on Wireless Communications*, vol. 19, no. 7, pp. 4657–4670, Jul. 2020.

[8] J. Jiao, Y. Sun, S. Wu, Y. Wang, and Q. Zhang, "Network Utility Maximization Resource Allocation for NOMA in Satellite-Based Internet of Things," *IEEE Internet of Things Journal*, vol. 7, no. 4, pp. 3230–3242, Apr. 2020.

[9] Z. Lin, M. Lin, J. Wang, T. d. Cola, and J. Wang, "Joint Beamforming and Power Allocation for Satellite-Terrestrial Integrated Networks With Non-Orthogonal Multiple Access," *IEEE Journal of Selected Topics in Signal Processing*, vol. 13, no. 3, pp. 657–670, Jun. 2019.

[10] S. Xie, B. Zhang, D. Guo, and B. Zhao, "Performance Analysis and Power Allocation for NOMA-Based Hybrid Satellite-Terrestrial Relay Networks With Imperfect Channel State Information," *IEEE Access*, vol. 7, pp. 136 279–136 289, 2019.

[11] S. M. Ivari, M. Caus, M. A. Vazquez, M. R. Soleymani, Y. R. Shayan, and A. I. Perez-Neira, "Power Allocation and User Clustering in Multicast NOMA based Satellite Communication Systems," in *ICC 2020 - 2020 IEEE International Conference on Communications (ICC)*, Jun. 2020, pp. 1–6, iSSN: 1938-1883.

[12] T. Ramírez and C. Mosquera, "Resource Management in the Multibeam NOMA-based Satellite Downlink," in *ICASSP 2020 - 2020 IEEE International Conference on Acoustics, Speech and Signal Processing (ICASSP)*, May 2020, pp. 8812–8816, iSSN: 2379-190X.

[13] L. Wang, Y. Wu, H. Zhang, S. Choi, and V. C. M. Leung, "Resource Allocation for NOMA based Space-Terrestrial Satellite Networks," *IEEE Transactions on Wireless Communications*, pp. 1–1, 2020.

[14] R. D. Yates, Y. Sun, D. R. B. I. au2, S. K. Kaul, E. Modiano, and S. Ulukus, "Age of information: An introduction and survey," 2020. [Online]. Available: https://arxiv.org/abs/2007.08564

[15] H. Yao, L. Wang, X. Wang, Z. Lu, and Y. Liu, "The Space-Terrestrial Integrated Network: An Overview," *IEEE Communications Magazine*, vol. 56, no. 9, pp. 178–185, Sep. 2018.

[16] E. Lagunas, A. Pérez-Neira, M. Martínez, M. A. Lagunas, M. A. Vázquez, and B. Ottersten, "Precoding With Received-Interference Power Control for Multibeam Satellite Communication Systems," *Frontiers in Space Technologies*, vol. 2, 5 2021.

[17] K. Chen and L. Huang, "Age-of-information in the presence of error," in *2016 IEEE International Symposium on Information Theory (ISIT)*, Jul. 2016, pp. 2579–2583.

[18] J. T. Gómez, M. Morales-Céspedes, A. G. Armada, and G. Hirtz, "Minimizing age of information on noma communication schemes for vehicular communication applications," in *2020 12th International Symposium on Communication Systems, Networks and Digital Signal Processing (CSNDSP)*, 2020, pp. 1–6.

[19] Ana Garcia-Armada, "SNR gap approximation for M-PSK-Based bit loading," *IEEE Transactions on Wireless Communications*, vol. 5, no. 1, pp. 57–60, Jan. 2006.

[20] D. Tse and P. Viswanath, *Fundamentals of Wireless Communication*, edición: 1 ed. Cambridge, UK ; New York: Cambridge University Press, Jul. 2005.

[21] S. M. R. Islam, M. Zeng, O. A. Dobre, and K.-S. Kwak, "Resource Allocation for Downlink NOMA Systems: Key Techniques and Open Issues," *IEEE Wireless Communications*, vol. 25, no. 2, pp. 40–47, Apr. 2018.